FULLY RESOLVED SIMULATION OF THE PHASE CHANGE PROCESS OF A LIQUID DROP

Vu Van Truong, Truong Viet Anh, Tran Xuan Bo, Truong Van Thuan

School of Transportation Engineering, Hanoi University of Science and Technology;
truong.vuvan1@hust.edu.vn, anh.truongviet@hust.edu.vn, bo.tranxuan@hust.edu.vn, thuan.truongvan@hust.edu.vn

Abstract - This paper presents a numerical investigation of the solidification process of a liquid drop on a cold solid surface. The drop is immersed in the computational domain with the presence of three phases: solid – liquid – gas. The Navier-Stokes and energy equations are used to solve the problem in which the interface separating different phases is represented by a front-tracking method. The interpolation technique is used to impose the non-slip boundary condition on the solid surface. The cold surface on which the drop is placed is the cause of solidification with the phase change interface propagating from the cold surface to the top of the drop. The numerical results of some typical cases that are compared with the available experimental ones indicate the accuracy of the numerical method used in this study.

Key words - Numerical simulation; phase change; liquid drop; front-tracking; three phases

1. Introduction

Understanding of the dynamics of a drop including phase change heat transfer is very important because of its wide range applications such as atomization, crystal growth, food processing and so on. In nature, one can find the solidification of water drops attaching to leaves, cable lines, wind turbine blades and aircraft wings. Accordingly, there have been many studies concerned with this solidification problem.

Experimentally, Enríquez et al. [1] dripped a water drop on a subzero temperature plate that caused the drop to freeze. Jin and co-workers [2] used a molecular tagging thermometry technique to capture the motion of the water–ice phase change interface during the solidification of a water drop on a cold plate. Recently, Zhang et al. [3] also paid attention to the freezing process of a water drop on a plate. Itoh and co-workers [4] used molten silicon, a semiconductor material, as a phase change material to growth crystallized silicon drops for solar cell applications. Satunkin [5] used molten silicon, germanium and indium antimonide to form solid drops and to find the growth angles at the tri-junction (where the three phases meet). A common interesting feature of all above-mentioned works is the formation of an apex at the top of the drop after complete solidification because of volume expansion and the effect of the growth angle.

Theoretically, Sanz [6] and Nauenberg [7] developed models to reproduce the evolution of the phase change and drop fronts of a drop solidifying on a cold plate. In another recent work, Zhang et al. [8] also theoretically investigated the freezing process of a water drop on a plate.

Concerning numerical simulations, a few studies have been done for the solidification problem of a liquid drop on a plate. For instance, the boundary integral method [9], the Galerkin finite element method [10] and the front-tracking method [11,12] have been used to investigate the dynamics of the phase change heat transfer of the drop solidification problem.

It is evident that the problem of a liquid drop solidifying on a cold plate has been getting more and more attractive. Thus, an accurate method for simulating the problem becomes very important. Accordingly, the present study presents a direct numerical method for simulations of a liquid drop solidifying on a cold plate. The methods used here are the front-tracking technique to represent the interface and an interpolation technique to deal with the non-slip boundary condition.

2. Numerical problem and governing equations

We consider an axisymmetric liquid drop placed on a cold plate whose temperature T_c is below the fusion temperature T_m of the drop liquid (Figure 1). Because of the cold plate, the solidifying front formed on the plate surface propagates upwards to the top of the drop. Initially, the liquid drop is assumed to be a section of a sphere with a volume denoted by V_0. The contact angle ϕ_0 is then defined at the plate. The growth angle at the tri-junction (i.e. triple point) at which three phases meet [12,13] is defined as

$$\phi_{gr} = \phi_s - \phi_l \tag{1}$$

where ϕ_s is the angle between the tangent to the solid–gas interface and the horizontal, and ϕ_l the tangent to the liquid–gas interface and the horizontal. Assuming all fluids (i.e. gas and liquid) to be incompressible, immiscible and Newtonian, the one-fluid formulation gives

$$\partial\left(\rho\mathbf{u}\right)/\partial t + \nabla\cdot\left(\rho\mathbf{u}\mathbf{u}\right) = -\nabla p + \nabla\cdot\mu(\nabla\mathbf{u} + \nabla\mathbf{u}^T) + \int_f \sigma\kappa\delta\left(\mathbf{x}-\mathbf{x}_f\right)\mathbf{n}_f\,dS + \rho\mathbf{f} + \rho\mathbf{g} \tag{2}$$

$$\partial\left(\rho C_p T\right)/\partial t + \nabla\cdot\left(\rho C_p T\mathbf{u}\right) = \nabla\cdot\left(k\nabla T\right) + \int_f \dot{q}\delta\left(\mathbf{x}-\mathbf{x}_f\right)dS \tag{3}$$

$$\nabla\cdot\mathbf{u} = 0 \tag{4}$$

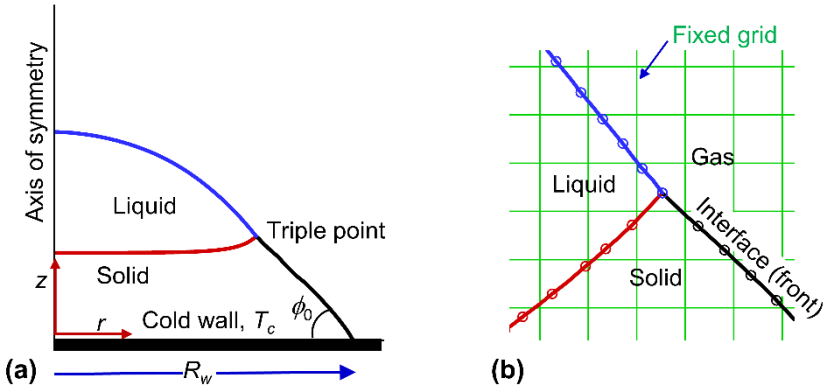

***Figure 1**. A liquid drop solidifying on a cold plate: (a) computational domain and (b) front-tracking representation*

Here, **u** is the velocity vector, p is the pressure, **g** is the acceleration induced by gravity, T is the temperature and **f** is the forcing term used to enforce the non-slip velocity boundary condition at the solid surface. ρ, μ, k and C_p are respectively the density, viscosity, thermal conductivity and heat capacity that are assumed constant in each phase. The Dirac delta function $\delta(\mathbf{x} - \mathbf{x}_f)$ is zero everywhere except a unit impulse at the interfaces $\mathbf{x}_f$ with f denoting interface. The superscript T denotes the transpose. At the liquid–gas interface, σ and κ are the interfacial tension coefficient and twice mean curvature, respectively. $\dot{q}$ is the heat source at the solidification interface, given as

$$\dot{q} = k_s \frac{\partial T}{\partial n}\bigg)_s - k_l \frac{\partial T}{\partial n}\bigg)_l \tag{5}$$

where the subscripts s, l and g (when available) represent solid, liquid and gas, respectively.

For some phase change materials such as water, silicon, and germanium, the density of the solid phase is different from that of the liquid phase, and thus change in volume occurs during solidification. Accordingly, Eq. (4) is rewritten as follows [12]

$$\nabla \cdot \mathbf{u} = \frac{1}{L_h}\left(\frac{1}{\rho_s} - \frac{1}{\rho_l}\right)\int_f \delta\left(\mathbf{x} - \mathbf{x}_f\right)\dot{q}dS \tag{6}$$

where L_h denotes the latent heat. The boundary conditions are as follows: symmetry at the left, full slip at the right, open at the top and non-slip at the bottom (Figure 1a).

3. Numerical method

To solve the problem, we use a front-tracking method for three phase simulations with an interpolation technique to treat the presence of the solid phase within the computational domain on which a uniformly distributed rectangular grid is constructed [14]. The spatial derivaties are descritized by a second-order central difference approximation. The time integration is approximated by a predictor-corrector scheme. The interface separating different phases is represented by connected points moving on the fixed grid (Figure 1b). We update the position of the liquid–gas and solid–liquid front points by

$$\mathbf{x}_f^{n+1} = \mathbf{x}_f^n + \mathbf{n}_f V_f \Delta t \tag{7}$$

where the superscripts n and n+1denote the current and next time levels. $\mathbf{n}_f$ is the unit vector normal to the interface. V_f, the velocity magnitude of the front point, is given as [15]

$$\mathbf{n}_f V_f = \sum d\left(r_x\right) d\left(r_y\right)\mathbf{u}_{ij}$$
$$\text{where } d\left(r\right) = \begin{cases} 1-r, & 0 < r < 1, \\ 1+r, & -1 < r < 0, \\ 0, & |r| \geq 1 \end{cases} \tag{8}$$

for the liquid–gas front, and $V_f = -\dot{q}/\left(\rho_s L_h\right)$ (9)

for the solid–liquid front with $\dot{q}$ calculated by a normal probe technique

$$\dot{q} = \frac{1}{h}\left[k_s\left(T_s - T_m\right) - k_l\left(T_m - T_l\right)\right] \tag{10}$$

where h is the grid spacing. T_s and T_l are the temperature of the solid and liquid near the phase change front at the solid and liquid points that are h away from the front. At the triple point, we impose a constant growth angle, ϕ_{gr} = constant [12]. Thereby, the solid–gas points are constructed.

To identify the phases as well as their fluid and thermal properties, we construct two indicator functions I_s (from the solid–liquid and solid–gas interfaces) and I_l (from the liquid–gas and solid–gas interfaces) whose values are specified as

$$\begin{cases} I_s = 0 \text{ in solid, and } I_s = 1 \text{ in liquid and gas} \\ I_l = 0 \text{ in solid and liquid, and } I_l = 1 \text{ in gas} \end{cases} \tag{11}$$

Accordingly, the values of the material properties such as ρ, μ, k and C_p (represented by φ) at every location in the domain are given by

$$\varphi = \left[\varphi_l I_s + \varphi_s\left(1 - I_s\right)\right] I_l + \varphi_g I_l \tag{12}$$

A more detailed description of the method used in this study can be found in [12,14].

4. Numerical parameters

We choose an equivalent radius of the drop $R_c = R = \left[3V_0/\left(4\pi\right)\right]^{1/3}$ as a scaling length. Here, V_0 is the

volume of the initial liquid drop. An alternative scaling length is the wetting radius R_w (Figure 1), i.e. $R_c = R_w$. The characteristic time scale is $\tau_c = \rho_l C_l R_c^2 / k_l$. The characteristic velocity scale is taken to be $U_c = R_c / \tau_c$. With these above choices, the dynamics of the problem is governed by the following dimensionless parameters (Prandtl number *Pr*, Stefan number *St*, Bond number *Bo*, Ohnesorge number *Oh*, dimensionless initial temperature θ_0, density ratios ρ_{sl} and ρ_{gl}, viscosity ratio μ_{gl}, thermal conductivity ratios k_{sl} and k_{gl}, heat capacity ratios C_{psl} and C_{pgl}):

$$Pr = \frac{C_{pl}\mu_l}{k_l}, St = \frac{C_{pl}(T_m - T_c)}{L_h}, Bo = \frac{\rho_l g R_c^2}{\sigma}, Oh = \frac{\mu_l}{\sqrt{\rho_l R_c \sigma}} \quad (13)$$

$$\theta_0 = \frac{T_0 - T_c}{T_m - T_c}, \rho_{sl} = \frac{\rho_s}{\rho_l}, \rho_{gl} = \frac{\rho_g}{\rho_l}, \mu_{gl} = \frac{\mu_g}{\mu_l} \quad (14)$$

$$k_{sl} = \frac{k_s}{k_l}, k_{gl} = \frac{k_g}{k_l}, C_{psl} = \frac{C_{ps}}{C_{pl}}, C_{pgl} = \frac{C_{pg}}{C_{pl}} \quad (15)$$

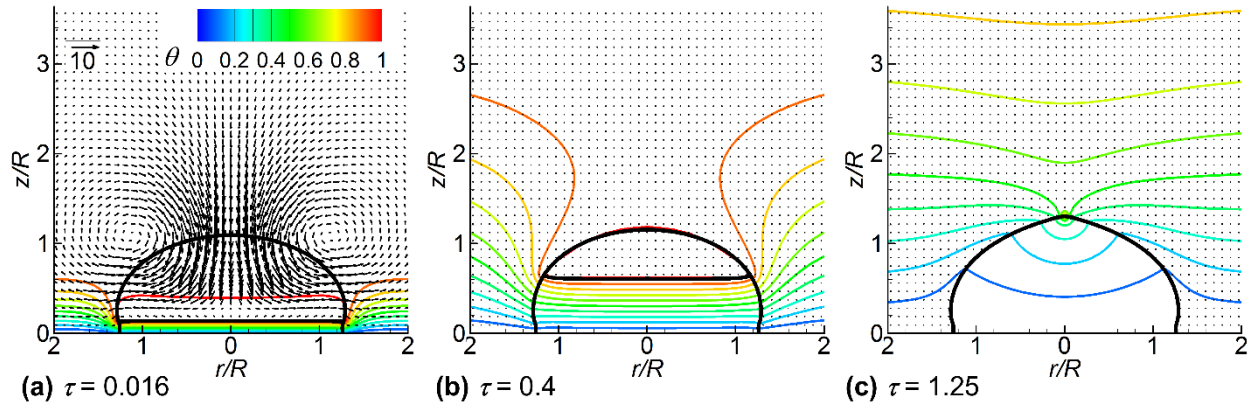

Figure 2. *Evolution of the solidifying front at different stages of solidification with the temperature contours (color) plotted every $\Delta\theta = 0.1$ and the velocity field normalized by U_c. R_c is equal to R. The parameters are shown in the text*

The temperature is non-dimensionalized as $\theta = (T - T_c)/(T_m - T_c)$. The dimensionless time is $\tau = t/\tau_c$.

5. Results and discussion

Figure 2 shows the temporal evolution of the solidification front with the temperature contours and the velocity field. The parameters for this calculation are *Pr* = 7.25, *St* = 0.104, *Oh* = 0.2, *Bo* = 2.0, ρ_{sl} = 0.9, $\rho_{gl} = \mu_{gl}$ = 0.05, k_{sl} = 4.0, k_{gl} = 0.05, C_{psl} = 0.5, C_{psl} = 0.24, $\phi_{gr} = 0^0$, θ_0 = 1 and $\phi_0 = 90^0$. At τ = 0.016 (Figure 2a), the gravity results in a downward flow at the center of the drop and deforms the drop, inducing counter clockwise circulations around the drop. This downward flow causes a reduction in the temperature field within the liquid phase while the temperature in the solid phase increases from the wall value ($\theta = \theta_c = 0$) at the wall to the fusion value ($\theta = \theta_m = 1$) at the solid–liquid interface. At a later time τ = 0.4, the gravity balances with the surface tension force holding the drop in a spherical shape, and thus no flow appears at this time (Figure 2b). Accordingly, the temperature in the liquid phase is almost at the fusion value. At τ = 1.25 (Figure 2c), almost all liquid has solidified, and the solidified drop has an apex at the top because of volume expansion (i.e., ρ_{sl} = 0.9) [12,14].

Figure 3 shows the temporal variation of the drop height and the drop volume for the case shown in Figure 2. This figure clearly shows the effect of the gravity at the beginning of solidification with a decrease in the height of the drop. Then, the surface tension force acting on the liquid–gas interface pushes the liquid–gas interface up to be against the gravity. Because the liquid is denser than the solid (ρ_{sl} < 1.0), the drop height and volume increase in time as the solidification proceeds as shown in Figure 3. After complete solidification, the volume of the solidified drop is about 1.1 times the volume of the initial liquid drop. A few phase change materials having such a feature, i.e. volume expansion upon solidification, include water, silicon and germanium [5]. However, most metals have the solid denser than the liquid and thus experience shrinkage upon solidification.

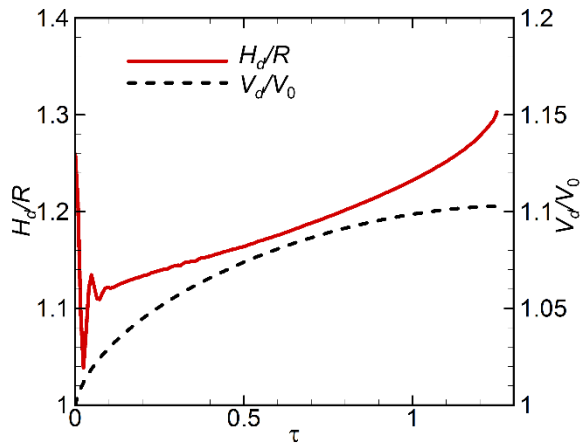

Figure 3. *Temporal variation of the solidifying front and the drop volume for the case shown in Figure 2*

To evaluate the capability of the method for computations of the solidification process of a drop, we perform a simulation of a water drop freezing on a cold plate and compared the results with the experiment of Zhang et al. [3], as shown in Figure 4. Experimentally, Zhang and co-workers [3] placed a water drop of 10 μL

on a horizontal wall that was kept at T_c = –16.5^{0}C, and used a photographic technique to capture the evolution of the ice–water phase change interface during freezing (bottom row in Figure 4). The corresponding Prandtl, Stefan and Bond numbers for this case are Pr = 7.5, St = 0.209 and Bo = 0.25, based on the properties of water and ice and $R_c = R$. The growth angle ϕ_{gr} is set to 0^0 [5]. The top row in Figure 4 shows the time sequence of the freezing of the drop yielded from the present computation. The comparison indicates that the computation result agrees quite well with the experimental data of Zhang et al. [3].

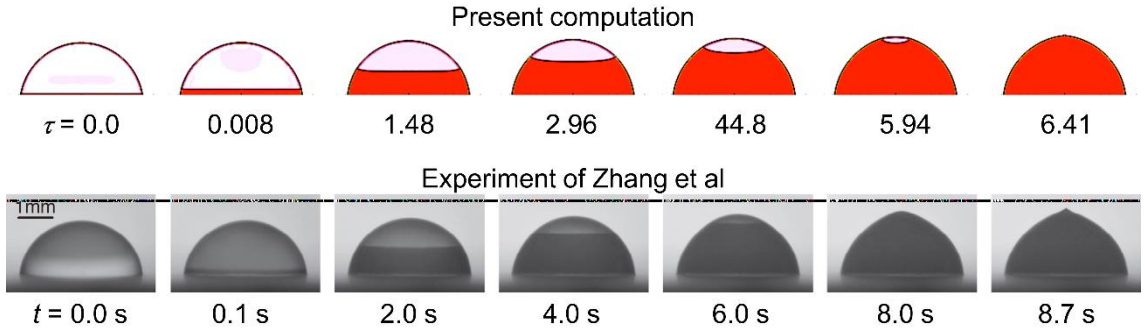

***Figure 4**. Evolution of the water–ice front at different stages of freezing in comparison with the experiments of Zhang et al. [3]. R_c is equal to R*

Figure 5 shows the evolution of the average height H_s of the freezing front for the case shown in Figure 4. The variation with respect to time of H_s indicates that the freezing rate is high at the beginning and near the end of the freezing process. This tendency is in accordance with Nauenberg's theoretical analysis [7]. As previously mentioned, water is a phase change material whose liquid density is higher than that of ice, and thus the drop expands in volume as the freezing process progresses, with a volume increment of about 10% after complete solidification, as shown in Figure 5. Figure 5 also confirms that the increase in the volume of the computational drop is in good agreement with the experimental result of Zhang et al. [3].

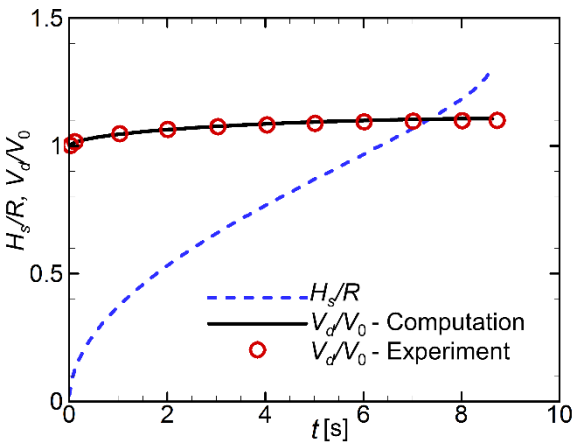

***Figure 5**. Temporal evolutions of the average height of the water–ice front H_s and of the volume of the drop V_d normalized by the volume of the initial liquid drop V_0. The cirles are data from the experiment of Zhang et al. [3]*

Silicon, a semiconductor material, also has a liquid phase denser than the solid phase, and thus experiences volume expansion upon crystallization. Figure 6 shows the evolution of the solid–liquid interface during the crystallization process of a molten silicon drop attaching to a cold wall. The main parameters for this computation are Pr = 0.013, St = 0.116, ρ_{sl} = 0.91 and ϕ_{gr} = 12^0, based on the properties of silicon [5]. Because of volume expansion and the effect of the growth angle, the crystallized silicon drop is very different from the initial molten one with an apex at the drop top. This crystallized drop shape agrees very well with the experimental drop shape (the most right frame in Figure 6) reported in Satunkin's work [5]. For more details of the comparison, see [11].

Figure 7 shows the evolution of the solidifying interface during the solidification process of an indium antimonide drop whose main parameters are Pr = 0.0255, St = 0.278, ρ_{sl} = 0.8 and ϕ_{gr} = 25^0. The corresponding solidified drop yielded from Satunkin's experiment [5] is present at the right of Figure 7. Because of the significant effects of the growth angle and volume change, the initial molten drop with a spherical cap solidifies to a very conical solid drop with a large increase in its height (the final height is more than two times higher than the initial height). This shape of the solidified drop is in good agreement with the experiment one reported by Satunkin [5]. For more details of the comparison, see [11].

Based on the comparisons with the available experiments, we can conclude that the method presented here can accurately capture the evolution of the solidifying drop attached to a cold wall.

6. Conclusion

We have presented a numerical method to simulate the solidification process of a liquid drop. The method is the front-tracking technique representing the interface by connected elements laid on a fixed rectangular grid. The drop with the presence of three phases (solid, liquid and gas) is immersed in the computational domain. The Navier-Stokes and energy equations are used in the entire domain with the solid treated by the interpolation technique. The propagation of the solid–liquid interface is calculated by the normal probe technique. The liquid drop initialy treated as a section of a sphere is placed on the plate whose temperature below the fusion value of the liquid causes the

solidifying front to form and move upwards. The numerical results show that the solidification process progresses fast at the begining, and the solidified drop forms a cone at the top of the drop in the case of volume expansion. The comparisons with the available experiments for various phase change materials including water, silicon, and indium antimonide show that the numerical method accurately captures the evolution of the solidification interface as wells as the drop shape after complete solidification.

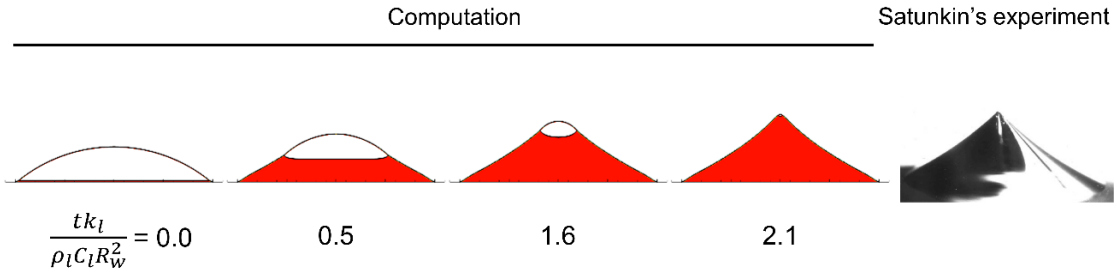

Figure 6. *The solidification process of a molten silicon drop in comparison with the crystallized drop of Satunkin [5]*

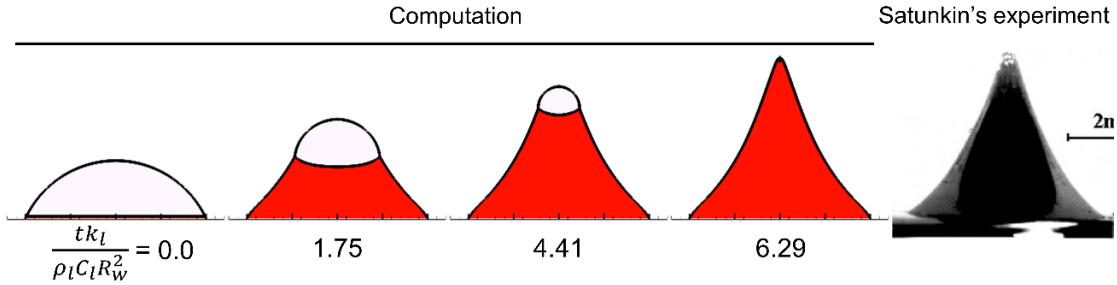

Figure 7*. The solidification process of a molten indium antimonide drop in comparison with the crystallized drop of Satunkin [5]*

Acknowledgments

This research is funded by Vietnam National Foundation for Science and Technology Development (NAFOSTED) under grant number 107.03-2017.01.

REFERENCES

[1] O.R. Enríquez, Á.G. Marín, K.G. Winkels, J.H. Snoeijer, Freezing singularities in water drops, *Phys. Fluids*. 24 (2012) 091102-091102-2.

[2] Z. Jin, X. Cheng, Z. Yang, Experimental investigation of the successive freezing processes of water droplets on an ice surface, *Int. J. Heat Mass Transfer*. 107 (2017) 906–915.

[3] X. Zhang, X. Wu, J. Min, Freezing and melting of a sessile water droplet on a horizontal cold plate, *Exp. Therm. Fluid Sci.* 88 (2017) 1–7.

[4] H. Itoh, H. Okamura, C. Nakamura, T. Abe, M. Nakayama, R. Komatsu, Growth of spherical Si crystals on porous Si3N4 substrate that repels Si melt, *J. Cryst. Growth*. 401 (2014) 748–752.

[5] G.A. Satunkin, Determination of growth angles, wetting angles, interfacial tensions and capillary constant values of melts, *J. Cryst. Growth.* 255 (2003) 170–189.

[6] A. Sanz, The crystallization of a molten sphere, *J. Cryst. Growth*. 74 (1986) 642–655.

[7] M. Nauenberg, Theory and experiments on the ice–water front propagation in droplets freezing on a subzero surface, *Eur. J. Phys.* 37 (2016) 045102.

[8] X. Zhang, X. Wu, J. Min, X. Liu, Modelling of sessile water droplet shape evolution during freezing with consideration of supercooling effect, *Appl. Therm. Eng.* 125 (2017) 644–651.

[9] W.W. Schultz, M.G. Worster, D.M. Anderson, Solidifying sessile water droplets, in: Interactive Dynamics of Convection and Solidification, *Kluwer Academic Publishers*, 2001: pp. 209–226.

[10] A. Virozub, I.G. Rasin, S. Brandon, Revisiting the constant growth angle: Estimation and verification via rigorous thermal modeling, *J. Cryst. Growth.* 310 (2008) 5416–5422.

[11] T.V. Vu, G. Tryggvason, S. Homma, J.C. Wells, H. Takakura, A front-tracking method for three-phase computations of solidification with volume change, *J. Chem. Eng. Jpn.* 46 (2013) 726–731.

[12] T.V. Vu, G. Tryggvason, S. Homma, J.C. Wells, Numerical investigations of drop solidification on a cold plate in the presence of volume change, *Int. J. Multiphase Flow*. 76 (2015) 73–85.

[13] T.V. Vu, Three-phase computation of solidification in an open horizontal circular cylinder, *Int. J. Heat Mass Transfer*. 111 (2017) 398–409.

[14] T.V. Vu, J.C. Wells, Numerical simulations of solidification around two tandemly-arranged circular cylinders under forced convection, *Int. J. Multiphase Flow*. 89 (2017) 331–344.

[15] G. Tryggvason, R. Scardovelli, S. Zaleski, *Direct numerical simulations of gas-liquid multiphase flows*, Cambridge University Press, Cambridge; New York, 2011.

(The Board of Editors received the paper on 25/02/2018, its review was completed on 28/3/2018)